Investigations of the Active Site of *Saccharomyces cerevisiae* Dolichyl-Phosphate-Mannose Synthase Using Fluorescent Labeled Dolichyl-Phosphate Derivatives†

Jun Xing,‡ W. Thomas Forsee,§ Ejvis Lamani,§ Sergei D. Maltsev,|| Leonid L. Danilov,|| Vladimir N. Shibaev,|| John S. Schutzbach,§ Herbert C. Cheung,‡ and Mark J. Jedrzejas*,§

Department of Biochemistry and Molecular Genetics and Department of Microbiology, The University of Alabama at Birmingham, 933 19th Street South, Birmingham, Alabama 35295-2041, and N. D. Zelinsky Institute of Organic Chemistry, Russian Academy of Sciences, 117913 Moscow, Russia

Received February 10, 2000; Revised Manuscript Received April 24, 2000

ABSTRACT: Dolichol-phosphate mannose (Dol-P-Man) is a key mannosyl donor for the biosynthesis of N-linked oligosaccharides as well as for O-linked oligosaccharides on yeast glycoproteins, and for the synthesis of the glycosyl-phosphatidylinositol anchor found on many cell surface glycoproteins. It is synthesized by Dol-P-Man synthase which is the only glycosyltransferase in the dolichol pathway that has been expressed as an active protein, solubilized and purified in large enough quantities for structural investigations. Earlier studies showed that the enzyme is closely associated with membranes of endoplasmic reticulum with unique lipid requirements for its maximal activity. This potential target of antibiotic therapy is now being investigated at the molecular level to establish information about the structure of the enzyme as well as determine the nature and properties of the enzyme−phospholipid interactions. In this paper, we have determined the activities of the fluorescent labeled dolichyl-phosphate derivatives as well as the intramolecular distances between amino acid residues near the active site and/or the fluorophores of the substrate derivatives using fluorescence energy resonance transfer. These results also show that the conserved consensus sequence is not required by Dol-P-Man synthase neither for the recognition of Dol-P nor for the catalytic activity.

Dolichyl-phosphate mannose (Dol-P-Man)[1] synthase (EC 2.4.1.83) is an endoplasmic reticulum resident membrane enzyme that catalyzes the formation of a key glycosyl donor in pathways for the synthesis of asparagine or N-linked oligosaccharides, O-linked oligosaccharides on yeast glycoproteins, C-linked mannose to tryptophan, and the glycosyl-phosphatidylinositol anchor of many cell surface glycoproteins (*1*−*3*). In the N-linked oligosaccharide assembly pathway, dolichyl-linked monosaccharides and oligosaccharides are synthesized by a concerted series of reactions catalyzed by glycosyltransferases found in membranes of the endoplasmic reticulum (ER). The lipophilic dolichol moiety functions to anchor the activated sugar residues, as well as the growing oligosaccharide chains, in membranes of the ER (*2*). The gene for Dol-P-Man synthase (DPM1) was initially cloned from *Saccharomyces cerevisiae* (*3*) but has more recently been cloned from other eukaryotes and higher organisms (*5*−*7*). DPM1 from *S. cerevisiae* codes for a protein of 267 amino acids with a molecular mass of 30.36 kDa. As first reported by Colussi et al. (*7*), the known sequences for Dol-P-Man synthase fall into two major classes, with enzymes from *S. cerevisiae*, *Ustilago maydis*, and *Trypanosoma brucei* comprising one class and enzymes from mammals, *Schizosaccharomyces pombe*, and *Caenorhabditis briggsiae* comprising a second group (Figure 1). Although within each class there is significant homology with at least 61% identity plus similarity, there is also approximately 39% overall identity plus similarity among all of the enzymes (*7*). One major difference between the 2 classes, however, is that the *S. cerevisiae* class of enzymes contains some additional 30 amino acids at the carboxyl terminus. This additional sequence includes a hydrophobic and/or potential membrane-spanning domain of 25 amino acids. Although the hydrophobic domain was originally proposed as a likely Dol-P recognition sequence, later results

† This work was supported by in part by U.S. Civilian Research and Development Foundation Grant RN1-404 (to M.J.J. and V.N.S.) and in part by an American Cancer Society Institutional Research Grant (to M.J.J.), and the time-resolved fluorescence instrumentation was supported by National Institutes of Health Grant RR10404 (to H.C.C.).

* To whom correspondence should be addressed at the Department of Microbiology, 933 19th St. S., 545 CHSB-19, The University of Alabama at Birmingham, Birmingham, AL 35295-2041. Telephone: (205)975-7627, Fax: (205)0975-5424, E-mail: jedrzejas@uab.edu, Web: www.microbio.uab.edu/faculty/jedrzejas.htm.

‡ Department of Biochemistry and Molecular Genetics, The University of Alabama at Birmingham.

§ Department of Microbiology, The University of Alabama at Birmingham.

|| N. D. Zelinsky Institute of Organic Chemistry, Russian Academy of Sciences.

[1] Abbreviations: DAMBI, 4-dimethylaminophenylazophenyl-4′-maleimide; Dol-P, dolichyl-phosphate; Dol-P-Man, Dol-P mannose; DTT, dithiothreitol; EDTA, ethylenediaminetetraacetic acid; ER, endoplasmic reticulum; FRET, fluorescence resonance energy transfer; GDP-Man, guanosine 5′-diphosphate-mannose; Hepes, *N*-(2-hydroxyethyl)piperazine-*N*′-2-ethanesulfonic acid; IAEDANS, (5-iodoacetamidoethyl)-aminonaphthalene-1-sulfonic acid; MPSA, multiple protein sequence analysis; Nbs_2, 5,5′-dithiobis(2-nitrobenzoic acid); NP-40, Nonident P40 [ethylphenylpoly(ethylene glycol)]; PE, phosphatidylethanolamine; Tris, tris(hydroxymethyl)aminomethane.

10.1021/bi0003240 CCC: $19.00
Published on Web 06/13/2000

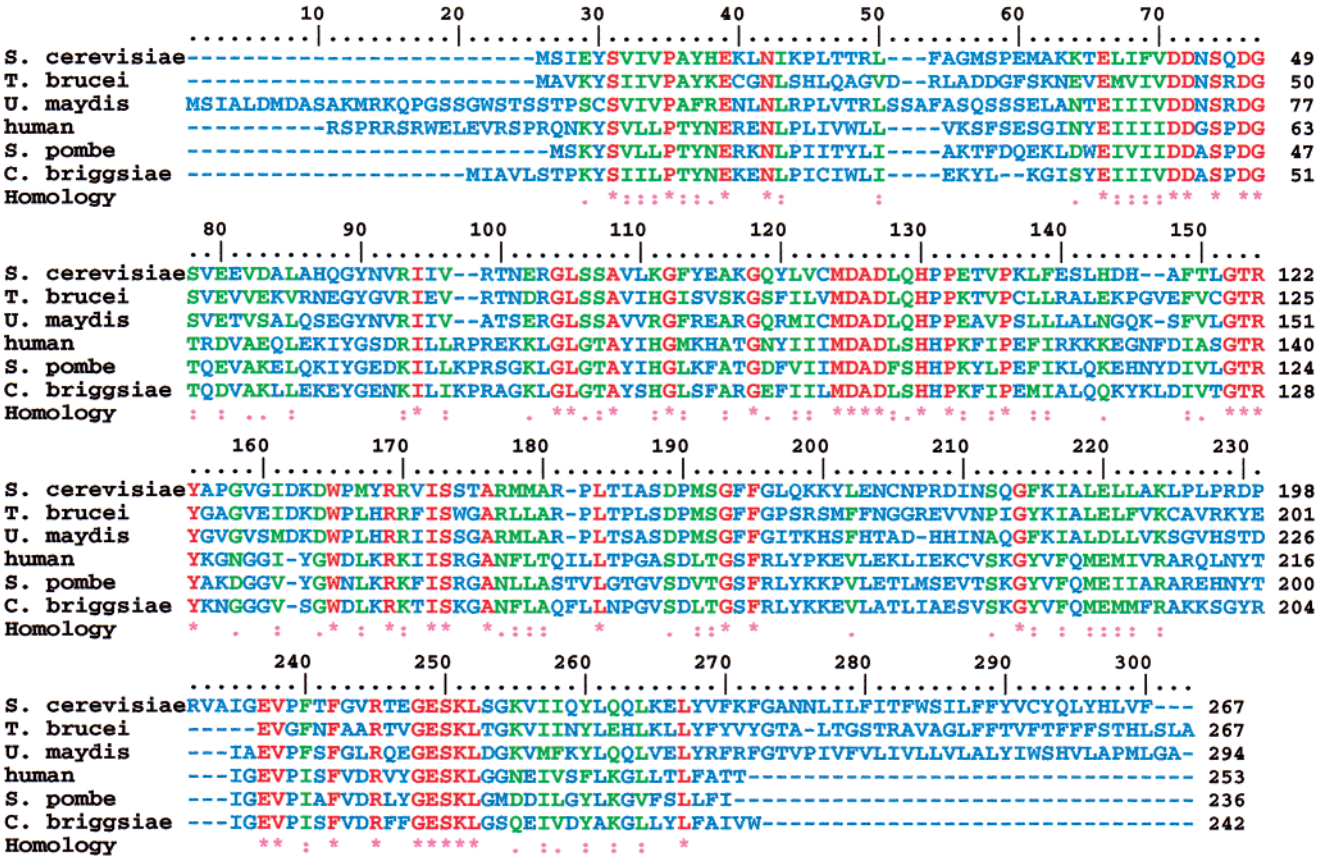

FIGURE 1: Sequence alignment of the *Saccharomyces cerevisiae* (GB_PL1:YSCDPM; top row), *Trypanosoma brucei* (PIR2:S70643; 2nd row), *Ustilago maydis* (GB_PL2:UMU54797; 3rd row), human (SP_HUMAN:015157; 4th row), *Schizosaccharomyces pombe* (GB_PL1:APAC31G6; 5th row), and *Caenorhabditis briggsiae* (GB_IN2:AF00787; bottom row) Dol-P-Man synthase (DPM1). The sequences were aligned were aligned using Multalin (*39*) and drawn using MPSA (*40*). Color coding for the alignment: red, single fully conserved residue; green, either 'strong' or 'weak' groups are fully conserved; blue, no particularity.

have demonstrated that the carboxyl terminus is not required for activity or for recognition of the hydrophobic polyisoprenoid substrate (*8*−*10*).

Dol-P-Man synthase is essential for yeast viability (*4*), and deficiencies of the enzyme in humans result in at least one form of the congenital disorders of glycosylation (CDG-1e) with concomitant severe clinical manifestations (*11*, *12*). The mammalian and yeast enzymes differ not only in size but also in kinetic properties, and they differ in requirements for activity in detergent or when reconstituted with a phospholipid matrix (*1*, *9*, *13*−*16*). Thus, Dol-P-Man synthase could serve as a potential target for antibiotic therapy of fungal infections as well as a locus for the correction of some deficiencies in CDG.

To obtain information about the mechanism and structure of the enzyme, the structural gene for yeast Dol-P-Man synthase was expressed in large amounts as an active protein in *Escherichia coli*, and the enzyme was purified to homogeneity (*9*, *17*). Site-directed mutagenesis has provided information concerning the interaction of Dol-P with the enzyme active site. Both Cys93 (*17*) and His100 (T. Forsee, P. Hughey, and J. Schutzbach, unpublished results) were shown to be near the binding site(s) for Dol-P and GDP-Man. Fluorescent labeled dolichyl derivatives have been synthesized (*18*) and shown to be substrates for the yeast Dol-P-Man synthase which are essentially indistinguishable from the natural substrate for this enzyme, Dol-P. A truncated yeast mutant enzyme, DPMΔ3, which lacks the putative transmembrane 25 C-terminal hydrophobic amino acids and is a likely model of the mammalian counterpart lacking these transmembrane residues, was used to investigate the active site using fluorescent resonance energy transfer (FRET). The distances between tryptophan and cysteine residues and the fluorescent labeled dolichyl derivatives were measured and analyzed.

MATERIALS AND METHODS

Enzyme Purification. The full-length DPM1 enzyme, its truncated form DPMΔ3 containing amino acids 1−238, and DPMΔ3C93S (same as DPMΔ3 but with Cys93 mutated to Ser) (see Results**)** forms of Dol-P-Man synthase were overexpressed, solubilized, and purified essentially as previously described (*9*). However, following chromatography on a 50 mL (2.5 × 10 cm) hydroxylapatite column (BioRad), the enzyme was further purified by gel filtration on 26/60 Superdex 75 (Amersham Pharmacia) and then by ion-exchange chromatography on 10/10 Mono-Q (Amersham Pharmacia). The gel filtration was performed using 10 mM Tris-HCl buffer at pH 7.4, 0.15 M NaCl, 1 mM DTT, 1 mM EDTA, and 0.08% Thesit using a column equilibrated with the same buffer. The Mono-Q step was performed using a 200 mL gradient from 0.15 to 0.50 M NaCl in 10 mM Tris-HCl (pH 7.4), 1 mM DTT, 1 mM EDTA, and 0.08% Thesit. The chromatographic fractions containing enzyme were combined and dialyzed for 18 h against 10 L of 10 mM Tris-HCl buffer, pH 7.4, containing 0.15 M NaCl, 1 mM DTT, 1

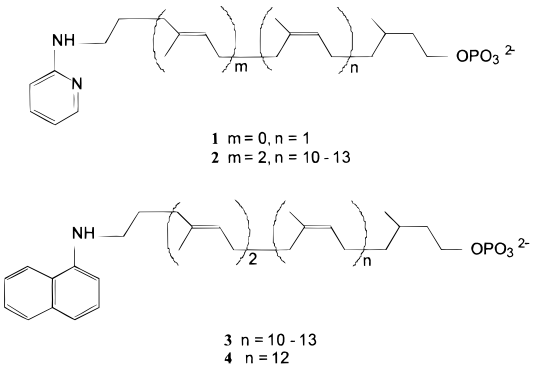

FIGURE 2: Chemical structures of fluorescent labeled dolichyl-phosphate derivatives: **1**, PyNH$(CH_2)_2-CS-P(NH_4^+)$; **2**, PyNH-$(CH_2)_2-T_2C_{10-13}S-P(NH_4^+)$; **3**, NafNH$(CH_2)_2-T_2C_{10-13}S-P(Na^+)$; **4**, NafNH$(CH_2)_2-T_2C_{12}S-P(NH_4^+)$.

mM EDTA, and 0.08% Thesit (v/v). The dialyzed enzyme was then concentrated to 10 mg/mL using a WM-10 membrane (Amicon). For the fluorescence studies, the enzyme was diluted to 1 mg/mL using 10 mM Tris-HCl, pH 7.5, 0.15 M NaCl, 1 mM DTT, with the concentration of NP-40 ranging from 0.2 to 2.0%. All procedures were performed either on ice or in a cold-room.

Enzymatic Assays. Dol-P-Man synthase was assayed utilizing a procedure that depends on the differential partitioning of the radioactive substrates and products in a two-phase scintillation mixture (*13*). The reaction mixture contained 0.1 M Hepes, pH 7.5, 0.15 M NaCl, 2.0% NP-40, 20 mM $MgCl_2$, 0.25 mM EDTA, 5 mM DTT, 0.04 mM GDP-[^{3}H]Man (0.1 μCi), and polyisoprenoid-P substrate (1−40 μg). Reactions were initiated by the addition of 8 ng of wild-type Dol-P-Man synthase, and the reactions were incubated at 25 °C for 5 min. The formation of mannosylated product was determined as described (*13*). This assay method was suitable for all the Dol-P analogues which contain long-chain hydrophobic acyl constituents. The water-soluble derivative, **1**, was assayed by a second procedure as previously described for the formation of phenyl phosphate mannose (*14*). The reaction mixture was as above except containing **1** (50−700 μg), and the reaction was incubated with 2 μg of Dol-P-Man synthase for 20 min. Formation of mannosylated product was detected utilizing paper chromatography of the reaction components as previously described (*14*). One unit of enzyme activity was defined as 1 μmol of mannose transferred from GDP-Man to polyprenyl-P per minute per milligram of enzyme.

Kinetic parameters such as K_m and k_{cat} were derived either by using the computer programs EZ-FIT (*19*) and ENZFIT (Elsevier-Biosoft) or by graphical methods. All methods resulted in determination of comparable kinetic parameters.

Synthesis of Fluorescent Labeled Dolichyl Derivatives. Dolichyl-phosphates containing fluorescent chromophores at the ω-terminus (**1**−**4**) (Figure 2) were synthesized and characterized as previously described (*18*).

All four compounds were stored at −20 °C under nitrogen in organic solvents: compound **1** in methanol, **2** in 4:1 (v/v) heptane/methanol mixture, **3** in 2:1 (v/v) benzene/methanol mixture, and **4** in 5:2 (v/v) hexane/2-propanol mixture. For the fluorescence studies, the organic mixture was evaporated under nitrogen flow, and the compounds were dissolved in buffer containing 10 mM Tris-HCl, pH 7.5, 0.15 M NaCl, 1 mM DTT, and 0.2% NP-40 (v/v). The amount of NP-40 in this buffer was kept to a minimum because of the NP-40 absorption of light around 280 nm which partially overlaps with the emission spectrum of a tryptophan residue.

Fluorescence Resonance Energy Transfer Studies. The DPMΔ3 and DPMΔ3C93S constructs of Dol-P-Man synthase were labeled at the single Cys93 with a 5-fold excess of the fluorescent sulfhydryl probe 1,5-IAEDANS [(5-iodoacetamidoethyl)aminonaphthalene-1-sulfonic acid, Molecular Probes] in a buffer containing 10 mM Tris-HCl at pH 7.5, 0.15 M NaCl, 1 mM DTT, and 0.2% NP-40. The reaction was carried out at 4 °C in the dark for 12 h, and unreacted probe was removed by exhaustive dialysis against the same buffer. The level of NP-40 was chosen to keep the enzyme soluble and minimize background absorption by the detergent in the range 290−300 nm. All fluorescence measurements were made in the same detergent-containing buffer. Similar conditions were used to label the Cys93 with the nonfluorescent probe DAMBI (4-dimethylaminophenylazophenyl-4′-maleimide). The degrees of labeling were found spectrophotometrically to be approximately 90%. The probes were obtained from Molecular Probes (Eugene, OR).

Steady-state fluorescence measurements were carried out on an ISS PC1 photon-counting spectrofluorometer, and emission spectra were corrected for variation of the detector with wavelength. Quantum yields were determined as in previous work (*20*), using L-tryptophan (quantum yield 0.14) as the standard for the tryptophan residue and quinine bisulfate in 0.1 N H_2SO_4 (quantum yield 0.71) for compound **3**. Fluorescence intensity decays were measured in the time domain with an IBH 5000 photon-counting lifetime system equipped with a very stable flash lamp operated at 40 kHz in 0.5 atm of hydrogen (*21*). All measurements were made at 20 ± 0.1 °C. Three donor−acceptor pairs were used to obtain a triangulation of the three sites: Trp133, Cys93, and the substrate binding site saturated with the fluorescent derivatives of dolichyl-phosphate. Trp133 was the energy donor for the two distances Trp133−Cys93 and the Trp133−Dol-P binding site (active site) using the fluorescent derivatives; the acceptors were IAEDANS covalently attached to Cys93 and the fluorescent derivatives **3** and **4** bound in the enzyme's active site. For the distance between the substrate site and Cys93, compound **3** was the donor, and the probe DAMBI linked to Cys93 was the acceptor. The transfer efficiency between Trp133 and the substrate site was determined by the steady-state donor intensity method (*20*). The transfer efficiencies between Trp133 and Cys93 and between the substrate binding site and Cys93 were determined by the donor lifetime method as previously described (*22*). For each donor−acceptor pair, the intensity decay data obtained from two samples, one containing the donor only and the other containing both donor and acceptor, were used to calculate the distribution of the donor−acceptor distances:

$$I_{DA}(r,t) = \sum_i \alpha_{Di} \exp\left[-\frac{t}{\tau_{Di}} - \frac{t}{\tau_{Di}}\left(\frac{R_o}{r}\right)^6\right] \quad (1)$$

$$I_{DA}(t) = \int_0^\infty P(r) I_{DA}(r,t)\, dr \quad (2)$$

where $I_{DA}(r,t)$ is the intensity decay of a donor−acceptor pair separated by a unique distance r, τ_{DA} are the decay times

of the donor in the absence of acceptor, α_{Di} are the associated amplitudes, and R_o is the Förster distance at which the transfer efficiency is 0.5. $I_{DA}(t)$ is the observed intensity decay for an ensemble of donor−acceptor pairs. $P(r)$ is the probability distribution of distances and is assumed to be a Gaussian function with the mean distance $\langle r \rangle$ and half-width hw = 2.354σ, where σ is the standard deviation of the distribution. R_o was determined for each donor−acceptor pair (*20*) under identical conditions as for FRET measurements, assuming random and rapid orientations of both donor and acceptor fluorophores. The distribution $P(r)$ was calculated from eq 2 using the program CFS_LS/GAUDIS (*22*). Since the degree of labeling of Cys93 with the acceptor IAEDANS was less than stoichiometric, the observed intensity decay of Trp133 contained a small contribution from donor fluorophores that did not participate in energy transfer. This contribution was corrected in the calculation. The labeling of Cys93 with the DAMBI acceptor was similarly less than stoichiometric for the transfer from compounds **3** and **4** bound in the active site of the enzyme to the acceptor site. The concentrations of these donor substrate analogues were adjusted so that only a small fraction of the active site was occupied. This condition ensured the absence of unbound donor molecules and the observed donor decay arose entirely from the bound donor.

Other Methods. Protein concentration was determined either by the Bradford protein assay (*23*) with bovine serum albumin as standard or by UV absorption at 280 nm using molar extinction coefficients of Dol-P-Man synthase that were calculated based on the amino acid sequence data (*24*). The multiple sequence alignment with hierarchical clustering for the enzyme from different sources was performed using Multalin program version 5.3.2 (*25*). The above aligned sequence data used to obtain Figure 1 were edited and analyzed with the Multiple Protein Sequence Analysis (MPSA) program (*26*).

RESULTS

Synthesis and Characterization of Fluorescent Substrates. Fluorescent labeled dolichyl-P derivatives **1**−**4** (Figure 2) were synthesized in order to study the active site properties of Dol-P-Man synthase enzyme. In these derivatives, the 2-aminopyridyl (PyNH-) or 1-aminonaphthyl (NafNH-) fluorophore group was present at the ω-terminal end of the isoprene chain, and the chain length of these polyisoprenoid compounds was varied (Figure 2) to probe the active site structure of the enzyme at multiple sites. For the preparation of **1**, racemic 2,3-dihydro-6*Z*-farnesyl acetate was used as a starting material. The Dol-P derivatives **2** and **3** represent mixtures of oligomer homologues (13−16 isoprene units), racemic at C-3. They were prepared from C_{70}−C_{85}-polyprenols of pine needles (*27*) with the use of nonstereoselective reduction of the double bond in the α-terminal isoprene unit (*28*). As shown by HPLC of the starting dolichols (*18*), the ratio of derivatives with n = 10, 11, 12, and 13 is 6:13:14:7. This mixture of compounds was very difficult to separate using the chromatographic techniques available. The derivative **4** is analogous to **3** but has a definite chain length of polyprenyl backbone composed of 15 isoprene units. Compound **4** was obtained in order to test the influence of the mixture of oligomers on the results obtained from the FRET studies. Only compound **1** was water soluble, whereas all other compounds were soluble only in organic solvents as described under Materials and Methods.

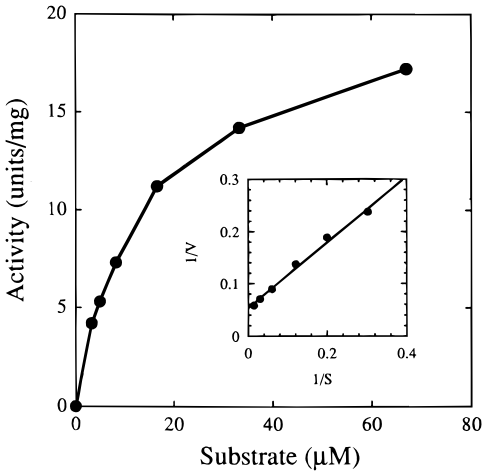

FIGURE 3: Activity of the DPM1 enzyme as a function of the fluorescent labeled Dol-P substrate derivative, **3**, concentration. Natural substrate, Dol-P, as well as fluorescent labeled dolichyl derivatives, **2**, **3**, and **4**, have similar activities. The assay was carried out as described under Materials and Methods.

These compounds were primarily designed to interact with a natural chromophore of the enzyme, Trp133, and second with chromophoric probes modifying Cys93 and Cys172 residues. The DPMΔ3 enzyme, which in comparison to the full-length DPM1 enzyme lacks the putative transmembrane 25 C-terminal hydrophobic amino acids, has only 1 Trp, Trp133, and 2 Cys, Cys93 and Cys172, residues whereas another mutant form of the enzyme, the DPMΔ3C93S double mutant, has only Trp133 and Cys93. The full-length, wild-type enzyme DPM1 has additional tryptophan, Trp251, and cysteine, Cys259, residues making it difficult to resolve selectively the fluorescence signal. Therefore, the DPMΔ3 mutant and the DPMΔ3C93S double mutant were advantageous for our studies and were used for the fluorescence analyses. The DPMΔ3C93S construct was used to distinguish between the Cys93 and Cys172 residues. Due to being buried deep inside the protein, the Cys172 residue was found not to be labeled by the probes used, IAEDANS and DAMBI. Therefore, the DPMΔ3 enzyme was later used for all fluorescent studies.

Enzyme Activity with Fluorescent Labeled Dolichyl Derivatives. The activity assays for all synthesized fluorescent labeled dolichol derivatives were performed using the wild-type, full-length DPM1 enzyme as described under Materials and Methods.

Compounds **2**−**4** synthesized to include the chromophoric fluorescent group were essentially indistinguishable in our activity assays from the natural substrate, Dol-P (Figure 3, Table 1). The K_m for the substrate analogues **2**, **3**, and **4** ranges from 11.6 to 14.5 μM**,** which closely compares to the 9.8 μM value for natural Dol-P. Additionally, k_{cat} values determined for these compounds range from 20.7 to 23.6 units/mg, which is in close agreement with the value of 17.6 units/mg for Dol-P (Table 1). Compound **1** had the shortest hydrophobic chain and, therefore, was also detected in the aqueous fraction of the biphasic enzymatic assay. Mannosylated compound **1** was also detected in this aqueous fraction and was separated out using paper chromatography followed by measurements of the radioactivity transferred

Table 1: Properties of Dol-P Substrate and Its Fluorescence Derivatives with the DPM1 Dol-P-Man Synthase

	Dol-P	**1**	**2**	**3**	**4**
K_m [K_I][a] (μM)	9.8 (0.8)	[2.0 mM]	11.6 (1.1)	14.5 (0.8)	11.7 (1.7)
k_{cat} (units/mg)[b]	17.6 (0.5)	NA[c]	23.6 (0.6)	20.7 (0.4)	22.4 (1.2)

[a] Compound **1** was water-soluble, and, therefore, instead of K_m, K_i was determined as described under Materials and Methods. [b] One unit of enzyme activity was defined as described under Materials and Methods. [c] NA, data not available.

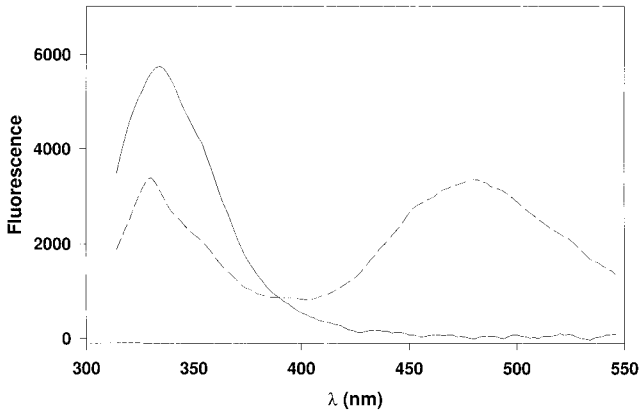

FIGURE 4: Fluorescence emission spectra of Trp133 of DPMΔ3 of Dol-P-Man synthase. The solid curve shows the tryptophan emission as a single band with the peak at 336 nm. The dashed curve is the spectrum obtained with the enzyme labeled at Cys93 with the acceptor probe IAEDANS. The protein concentration was 1 μM in both samples. The large quenching of the trytophan emission intensity is accompanied by the appearance of the sensitized emission of the acceptor probe. Both samples were excited at 298 nm.

in the form of [^{3}H]Man. This mannosylated reaction product migrated on the chromatographic paper similarly to phenyl phosphate (*14*, and data not shown). Due to this water solubility of compound **1**, only K_i was determined instead of K_m and k_{cat} as was done for the other three compounds, **2**−**4**, and Dol-P (Table 1). In summary, all compounds were shown to be substrates for Dol-P-Man synthase as they were acceptors for Man originating from the GDP-Man substrate. The binding and catalytic properties to the enzyme are uniform throughout compounds **2**−**4** and are comparable to binding of Dol-P (considering experimental errors). Somewhat different properties of compound **1** emphasize the importance of the hydrophobic tail of Dol-P in the catalysis performed by Dol-P-Man synthase.

Fluorescence Resonance Energy Transfer. The DPMΔ3 construct and/or the double mutant, DPMΔ3C93S, were used for the determination of intersite distances by FRET between Trp133 and Cys93, between Trp133 and the active site, and between the active site and Cys93. Figure 4 shows the emission spectra of Trp133 in the absence and presence of the acceptor IAEDANS attached to Cys93. The emission peak at 336 nm suggests that the tryptophan is located in an environment that is slightly less polar than water. In the presence of the acceptor, the peak intensity is more than 50% quenched, accompanied by the appearance of a second broad band with the maximum in the 470 nm region. This second band arises from the emission of the attached AEDANS probe. These reciprocal changes are an indication of energy transfer from the donor tryptophan to the acceptor AEDANS. The intensity decay of this tryptophan in the absence of

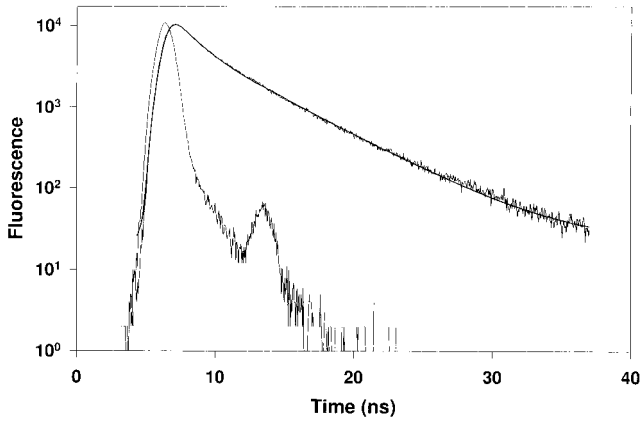

FIGURE 5: Intensity decay of the Trp133 in DPMΔ3 of Dol-P-Man synthase. The narrow sharp peak on the left is the lamp profile. The tracing was fitted to a sum of three exponential terms with a χ_R^2 value of 1.15. Excitation = 295 nm and emission = 340 nm. See text for the values of the three recovered lifetimes.

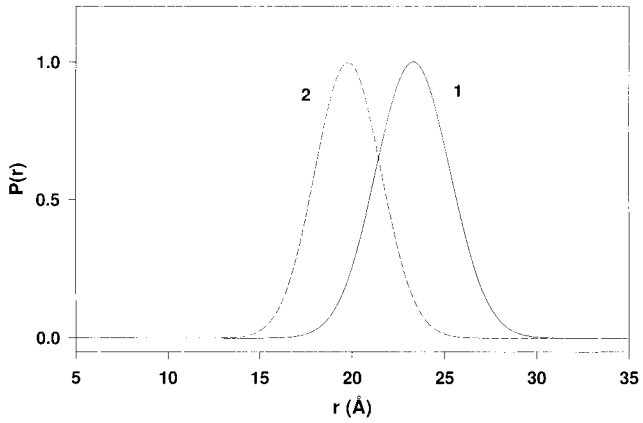

FIGURE 6: Distribution of the distances Trp133−Cys93 in DPMΔ3 of Dol-P-Man synthase. The donor was Trp133, and the acceptor was AEDANS covalently attached to Cys93. Curve 1, the distribution determined in the absence of substrate (χ_R^2 = 1.04); curve 2, in the presence of a 10-fold excess of the substrate Dol-P (χ_R^2 = 1.34). The two distributions were peak-normalized to facilitate comparison.

energy transfer is characterized by a sum of three exponential terms (Figure 5), with lifetimes 6.87 (8%), 3.32 (32%), and 0.89 (61%) ns. The intensity-weighted mean lifetime is 3.61 ns, a value consistent with a local environment not highly polar, which is also suggested by the steady-state emission spectrum. Since the Trp133 is not located in the membrane-spanning domain of the enzyme, the fluorescence results suggest that this residue is unlikely on the protein surface, but not highly shielded from collision with solvent.

Using the intensity decay parameters of the Trp133 obtained in the absence and presence of the acceptor, we calculated the mean intersite distance between Trp133 and Cys93 and the distribution of the distances both in the absence and in the presence of bound substrate. The two distribution curves are shown in Figure 6, and the distance parameters are given in Table 2. In the absence of bound substrate, the mean intersite distance is 22.3 Å. This value refers to the separation between the indole ring of the Trp133 and the center of the naphthalene moiety of the probe attached to the Cys93. The presence of bound substrate induced a decrease of 3.3 Å in the mean distance and a small decrease in the half-width of the distribution. The

Table 2: Distance Parameters in Dol-P-Man Synthase[a]

distance	R_o (Å)	r (Å)	$\langle r \rangle$ (Å)	hw (Å)	χ_R^2
Trp133−Cys93, no substrate	21.2		22.3 ± 0.1	5.0 ± 0.1	1.04
Trp133−Cys93 with Dol-P	21.2		19.0 ± 0.2	4.1 ± 0.2	1.34
Trp133−compound **3**, fluorophore	17.5	17.8 ± 1.3			
Trp133−compound **4**, fluorophore	19.3	18.6 ± 1.0			
Cys93−compound **3**, fluorophore	41.4		35.5 ± 0.4	6.3 ± 0.4	1.08

[a] These results were determined with mutant DPMΔ3. The distances Trp133−Cys93 and active site **3** were determined using lifetime data to recover the distribution of the distances, and the Trp133−active site distances were determined by the steady-state intensity method. R_o is the Förster critical distance, $\langle r \rangle$ is the mean distance from the distribution, hw is the half-width of the distribution, and r is the single distance calculated from the steady-state data. The goodness of the distribution fits is given by the χ_R^2 values. The uncertainties for $\langle r \rangle$ and hw correspond to the uncertainties associated with an increase in the normalized χ_R^2 value of one standard deviation (*F*-static), and these uncertainties define the possible errors associated with the determination of the parameters from the distance distribution. The uncertainties in r are the errors associated with measurements of the parameters for the calculation of the single distance and were calculated from the theory of propagation of random errors. The Trp133 lifetime data were obtained with excitation at 295 nm, and its emission was isolated at 340 nm. The corresponding wavelengths for the lifetime data of **3** were 340 and 410 nm, respectively.

measurement with bound substrate was performed in the presence of a 10-fold excess of the substrate, estimated from the experimental value of K_d to be sufficient to saturate all sites. The observed changes in both the mean distance and the half-width would be underestimates if a small fraction of the active site was not saturated.

To establish the extent to which the two mean distances can be considered distinct, we calculated the χ_R^2 surfaces for the two distances as in previous work (*21, 29*). These two surfaces were sharp and intersected at χ_R^2 values considerably above the values with random noise in 68% of repetitive measurements. This analysis shows that the two distance distributions shown in Figure 6 were distinct and the two mean distances were significantly different. The two distributions are relatively narrow in comparison with the distributions of intersite distances of some proteins that show half-widths in the range 8−12 Å (*21*−*22, 30*). Although no theoretical model is available to describe the separation between two residues for the native conformation of proteins (*31*), results from mellitin suggest that narrow distributions (1−3 Å) are indicative of highly constrained conformations (*32*). The present results would suggest that the region of Dol-P-Man synthase between residues Cys93 and Trp133 is likely constrained even though this region is not membrane-spanning. Although the decrease in the half-width induced by substrate binding is small, an analysis of the χ_R^2 surfaces suggests that the change was likely beyond random error. Thus, substrate binding may increase slightly the conformational constraint of this region of the enzyme. Since Cys93 is believe to be close to the active site (*38*), it is not surprising that the distance parameters are sensitive to substrate binding.

Figure 7 shows the fluorescence excitation and emission spectra of the two naphthalene derivatives of dolichyl sulfate (compounds **3** and **4**). Both have essentially identical emission spectra and quantum yields with peaks near 407 nm. Although one derivative has a narrower excitation band, both have similar spectral shapes and identical excitation peaks at 341 nm. There is an extensive spectral overlap between the emission band of the Trp133 of the enzyme and these excitation bands (Figures 4 and 7). This overlap indicates that the Trp133 is a good donor of resonance energy to the fluorescence substrate analogues, allowing determination of the separation between the Trp133 and bound substrates at the active site. This Trp133−active site distance was determined with both derivatives bound to the active site, using the steady-state method. For this set of measurements, a 40-fold excess of substrate analogues was used to ensure that the active site was fully saturated. Compounds **3** and **4** have detectable emission upon excitation at 295 nm. The intensity decay of this emission contributed to the observed intensity decay of Trp133 in the Trp133−substrate analogue system. This contribution cannot be corrected from the decay curve but was readily corrected in steady-state measurements of the Trp133 intensity. For this reason, the steady-state method was used. The results from these measurements are also listed in Table 2. The distances determined with the two analogues are only 0.8 Å apart, with a mean of 18.2 Å. These results were expected since the two analogues differ on average by only one isoprene unit. The determined distances are the separation between the Trp133 indole ring and the naphthalene moiety linked to the ω-end of the long isoprene chain bound to the active site. Because of the length of the isoprene chain, the determined distances may not readily suggest where the acceptor moiety is located within the active site pocket.

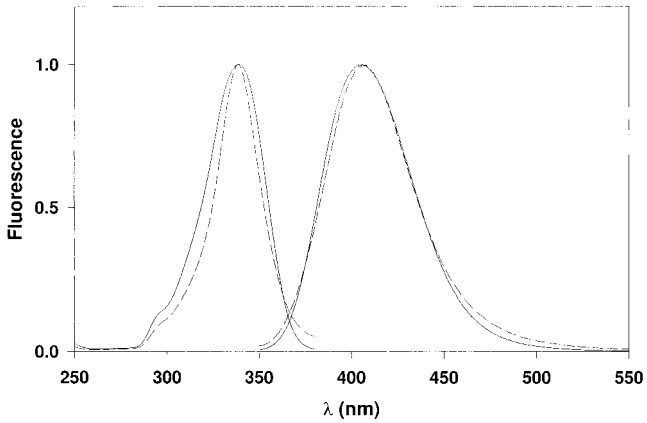

FIGURE 7: Fluorescence spectra of compounds **3** and **4**. The two spectra on the left are excitation spectra, and the two on the right are emission spectra. Solid curve, **4**; dashed curve, **3**. The spectra are peak-normalized for easy comparison. The excitation spectra were obtained with the emission monochromators set at 410 nm, and the emission spectra were obtained with excitation at 340 nm.

The intensity decay of **3** bound to DMPΔ3 synthase followed a triexponential decay law (data not shown), with three lifetimes (13.9, 5.0, and 0.63 ns; corresponding amplitudes 26, 15, and 59%, respectively). In the presence of the acceptor DAMBI attached to the Cys93, the two fastest components of the decay were quenched with a redistribution of the amplitudes toward the fastest component. These data

were used to determine the distribution of the distances between the bound donor at the active site and DAMBI attached to the Cys93. These results are given in Table 2.

Two additional fluorescent Dol-P derivatives were explored as potential energy acceptors from the Trp133. They contained a 2-aminopyridine moiety at the ω-end of the isoprene chain, compounds **1** and **2**. The peak of the longest wavelength absorption band of compound **1** is 307 nm, and this band has a very small overlap with the emission band of Trp133, making energy transfer between these two fluorophores inefficient. Additionally, its high absorbance at the excitation wavelength of the Trp133 poses a large inner filter effect, thus making it difficult to measure energy transfer from the tryptophan to the compound. Compound **2** has similar absorption properties with an absorption maximum at 315 nm, and the spectral properties similarly make it difficult for energy transfer studies. Therefore, no FRET information was obtained using these compounds.

DISCUSSION

Enzyme Activity with the Fluorescent Dol-P Derivatives. Compound **1** has very low affinity for the enzyme and is only a substrate at approximately 3 orders of magnitude greater than the long-chain dolichyl-phosphates (Table 1). Since the water-soluble and the organic-soluble dolichyl-phosphate-mannose products are analyzed separately, compound **1** acts essentially as a compatible inhibitor of Dol-P, and hence its affinity (K_i) can be directly quantified. Although the K_m of this compound was not directly determined, it was found to be a substrate at a comparable concentration range to phenyl-P, which was previously determined to be 2.3 mM (*14*). Compounds **2**−**4** had a longer polyisoprene chain length with the chromophoric groups at the ω-terminal end. They were water-insoluble, and their activity was found to be very similar to the natural Dol-P-Man synthase substrate, Dol-P (Table 1).

Specificity of Yeast Dol-P-Man Synthase for Dol-P. Yeast Dol-P-Man synthase, in common with similar enzymes from other sources, is known to show rather loose specificity toward the structure of the polyprenyl residue of Dol-P. Both *(S)*-(natural) and *(R)*-enantiomers of Dol-P were shown to serve as a substrate for the enzyme (*33*, *34*). It was found to be able to interact with a wide range of phosphates derived from short-chain polyprenols (*35*), retinol (*36*), phytanol or 3-methyloctadecanol (*37*), and phenol (*14*). Such properties of the enzyme allow employment for these studies of more readily available racemic derivatives of Dol-P with different chain length.

Active Site Analysis. Based on the earlier chemical modification studies followed by site-directed mutagenesis, both Cys93 (*38*) and His100 (T. Forsee, unpublished results) appear to be near the binding sites for Dol-P and also GDP-Man. Our studies using fluorescent labeled dolichyl derivatives (*18*) using the mutated yeast enzyme, DPMΔ3 and DPMΔ3C93S (*38*), have provided additional information concerning the interaction of Dol-P with the enzyme active site. The FRET analysis showed that all compounds synthesized bind to the above enzyme constructs which confirms earlier suggestions/observations (*9*) that the conserved consensus sequence at the C-terminal, hydrophobic part of Dol-P-Man synthase is not required by the enzyme for the recognition of Dol-P nor for the catalysis.

The observed mean distance between Trp133 and Cys93 is considerably shorter than expected for an elongated α-helical segment and suggests that the two residues are located in different secondary structural elements. The side chain of the Trp residue is not likely to be on the protein surface, but it is also not likely to be inserted deep into the interior of the enzyme as well as surrounded by other highly nonpolar side chains. If DMPΔ3 is assumed to be globular and spherical with a hydration of not more than 0.4 g of H_2O/g of protein, its dimensions would be in the range 40−43 Å, a factor of 2 larger than the observed Trp133−Cys93 distance. Any change in the tertiary structure of the segment connecting the two residues can result in a change in their separation. This structure is perturbed by the binding of Dol-P to the active site as reflected by a decrease of 3 Å in the Trp133−Cys93 mean separation. FRET data also suggest that, in the absence of bound substrate, this segment is likely constrained. This constraint appears to increase slightly upon saturation of the active site. It is not known if this global conformational change arises from movement of both residues toward each other, or movement of only one residue toward the other. Additional studies are needed to establish whether the effect of substrate binding is also transmitted to other regions of the enzyme.

The two distances from the active site to Trp133 and Cys93 do not provide insights as to whether saturation of the active site may result in perturbation of the positions of the indole ring of the attached acceptor probe because the determination was made with the bound substrate. These distances do allow triangulation of the three sites when the active site is saturated with fluorescence derivatives of the substrate. A simple geometry that is consistent with the distance results is an approximate isosceles triangle in which the base (35.5 Å) connects the active site and Cys93 and Trp133 is at the vertex. This vertex angle is likely $\leq 160°$. In the absence of a high-resolution structure of DMPΔ3, these low-resolution results are useful for visualization of the local topography of the active site region.

Previous work has shown that the Cys93 residue is near or at the active site of the Dol-P-Man synthase (*38*). Furthermore, both the hydrophilic glycosyl donor GDP-Man and the hydrophobic acceptor Dol-P were found to protect the enzyme against inactivation by the site-specific probe 5,5′-dithiobis(2-nitrobenzoic acid) (Nbs_2), suggesting the Cys93 is in proximity to the likely binding sites for both substrates (*38*). The distances between Cys93, Trp133, and the fluorophore of the derivatized substrates are consistent with this possibility. The distance between the active center of compound **3**, the phosphate end, and the fluorophore at its ω-end can be approximated, based on the standard lengths of single and double C−C bonds, to be at maximum $\sim$ 45 Å but is likely to be somewhat shorter due to folding of the long polyisoprene chain. Considering the measured fluorophore−Cys93 distance of 35.5 Å, this Cys residue can be placed within $\sim$10 Å from the phosphate group (active center) of compound **3** as well as in similar proximity of the active site of the synthase with the ω-terminus located closer to Trp133.

Yeast and Mammalian Dol-P-Man Synthase. The yeast DPM1 gene encodes a Dol-P-Man synthase with a transmembrane carboxyl terminus containing a putative dolichol binding site (*4*, *38*). In mammalian cells, the formation of

Dol-P-Man appears to require two gene products: a homologue of DPM1 which lacks a hydrophobic transmembrane domain (Figure 1), and a second gene product which is defective in Lec15 mutant cells (*39*−*40*). Purified yeast Dol-P-Man synthase is active in the presence of detergents such as NP-40, and when reconstituted with phospholipids, it is optimally active in unsaturated species of PE or with lipid mixtures that form destabilized bilayers (*9*). Wild-type yeast Dol-P-Man synthase demonstrated apparent K_ms for Dol-P of 9.8 μM when assayed in detergent, and 2.7 μM in PE (*9*). Significantly, mutant forms of the yeast enzyme either which lack the carboxyl terminus or in which critical residues in this region have been replaced demonstrated much lower affinity for Dol-P (apparent K_m values of 45−195 μM) in detergent, but retained high affinity for the polyisoprenoid substrate when assayed in PE. Interestingly, liver Dol-P-Man synthase, which was purified 880-fold (and presumably no longer contained the Lec15 gene product), was no longer active in detergents, but was fully active in PE (*13*).

Since the DPMΔ3 yeast Dol-P-Man synthase mutant is very similar to its mammalian counterpart, our structural studies of DPMΔ3 reported here should likely be directly relevant to the properties of the mammalian enzyme. Additionally, the procedures developed here should be useful for investigating this system as well as other enzymes in the dolichol pathway.

Glycosylation and Disease. Recently, deficiency in Dol-P-Man synthase was directly linked with carbohydrate-deficient glycoprotein syndrome, type IV (*41*−*43*). Genetic disorders compromising the function of the synthase have therefore direct clinical relevance. Also, glycosylation changes are a common observation in diseases such as cancer (*44*, *45*). Careful consideration is, however, needed since sometimes the cause of glycosylation changes may be secondary to the disease. Inhibition of glycoprotein biosynthesis may be used to reprogram glycoprotein biosynthesis and to modulate the biological functions of diseased cells. Inhibitors could be designed to target specific cells and specific steps in the biosynthetic pathways to correct genetic defects or modulate the growth of malignant cells. Additionally, Dol-P-Man synthase is essential for yeast viability, and as shown above the yeast enzyme differs in many properties from the mammalian enzyme (Figure 1); it may be possible to identify specific inhibitors of the fungal enzyme that will not affect human cells and therefore will be potentially useful antifungal agents. Similar inhibitors could be produced to target analogous enzymes in parasites and bacteria.

ACKNOWLEDGMENT

We thank R. Brandon Mewbourne for his help and assistance.

REFERENCES

1. Orlean, P. (1992) *Biochem. Cell Biol. 70*, 438−447.
2. Schutzbach, J. S. (1997) *Glycoconjugate J. 14*, 175−182.
3. Doucey, M., Hess, D., Cacan, R., and Hofsteenge, J. (1998) *Mol. Biol. Cell 9*, 291−300.
4. Orlean, P., Albright, C., and Robbins, P. W. (1988) *J. Biol. Chem. 263*, 17499−17507.
5. Mazhari-Tabrizi, R., Eckert, V., Blank, M., Muller, R., Mumberg, D., Funk, M., and Schwarz, R. T. (1996) *Biochem. J. 316*, 853−858.
6. Zimmerman, J., Specht, C., Cazares, B. X., and Robbins, P. W. (1996) *Yeast 12*, 765−771.
7. Colussi, P. A., Taron, C. H., Mack, J. C., and Orlean, P. (1997) *Proc. Natl. Acad. Sci. U.S.A. 94*, 7873−7878.
8. Albright, C. F., Orlean, P., and Robbins, P. W. (1989) *Proc. Natl. Acad. Sci. U.S.A. 86*, 7366−7369.
9. Schutzbach, J. S., Zimmerman, J. W., and Forsee, W. T. (1993) *J. Biol. Chem. 268*, 24190−24196.
10. Schutzbach, J. S. (1994) *Acta Chem. Pol. 41*, 269−274.
11. Imbach, T., Schenk, B., Schollen, E., Burda, P., Stutz, A., Grunewald, S., Bailie, N. M., King, M. D., Jaeken, J., Matthijs, G., Berger, E. G., Aebi, M., and Hennet, T. (2000) *J. Clin. Invest. 105*, 233−239.
12. Kim, S., Westphal, V., Srikrishna, G., Mehta, D. P., Peterson, S., Filiano, J., Karnes, P. S., Patterson, M. C., and Freeze, H. H. (2000) *J. Clin. Invest. 105*, 191−198.
13. Jensen, J. W., and Schutzbach, J. S. (1985) *Eur. J. Biochem. 153*, 41−48.
14. Jensen, J. W., and Schutzbach, J. S. (1986) *Carbohydr. Res. 149*, 199−208.
15. Jensen, J. W., and Schutzbach, J. W. (1988) *Biochemistry 27*, 6315−6320.
16. Schutzbach, J. S., and Zimmerman, W. (1992) *Biochem. Cell Biol. 70*, 460−465.
17. Schutzbach, J. S., and Forsee, W. T. (1993) *Glycobiology 3*, 530.
18. Shibaev, V. N., Vesolovsky, V. V., Lozanova, A. V., Maltsev, S. D., Danilov, L. L., Forsee, W. T., Xing, J., Cheung, H. C., and Jedrzejas, M. J. (2000) *Bioorg. Med. Chem. Lett. 10*, 189−192.
19. Perrella, F. W. (1988) *Anal. Biochem. 174*, 437−447.
20. Xing, J., and Cheung, H. C. (1995) *Biochemistry 34*, 6475−6487.
21. She, M., Dong, W.-J., Umeda, P. K., and Cheung, H. C. (1998) *J. Mol. Biol. 281*, 445−452.
22. Dong, W.-J., Chandra, M., Xing, J., She, M., Solaro, R. J., and Cheung, H. C. (1997) *Biochemistry 36*, 6754−6762.
23. Bradford, M. M. (1976) *Anal. Biochem. 72*, 248−254.
24. Pace, C. N., Vajdos, F., Fee, L., Grimsley, G., and Gray, T. (1995) *Protein Sci. 4*, 2411−2423.
25. Corpet, F. (1988) *Nucleic Acids Res. 16*, 10881−10890.
26. Blanchet, C., Geourjon, C., and Deleage, G. (1999) *Multiple Protein Sequence Analysis*, IBCP, CNRS UPR 412, Lyon, France.
27. Ibata, K., Mizuno, M., Tanaka, Y., and Kageyu, A. (1984) *Photochemistry 23*, 783−786.
28. Veselovsky, V. V. (1999) *Izv. Akad. Nauk. Ser. Khim.* 1009−1011.
29. Lakowicz, J. R., Gryczynski, I., Cheung, H. C., Wang, C.-K., Johnson, M. L., and Josh, N. (1988) *Biochemistry 27*, 9149−9160.
30. Cheung, H. C., Wang, C.-K., Gryczynski, I., Wiczk, W., Laczko, G., Johnson, M. L., and Lakowicz, J. R. (1991) *Biochemistry 30*, 5238−5247.
31. Wu, P., and Brand, L. (1992) *Biochemistry 31*, 7939−7947.
32. Lakowicz, J. R., Gryczynski, I., Wiczk, W., Laczko, G., Prengergast, F. G., and Johnson, M. L. (1990) *Biophys. Chem. 36*, 99−115.
33. Chojnacki, T., Palamarczyk, G., Jankowski, W., Krajewska-Rychlik, I., Szkopinska, A., and Vogtman, T. (1984) *Biochim. Biophys. Acta 793*, 187−192.
34. Palamarczyk, G., Vogtman, T., Chojnacki, T., Bause, E., Mizuno, M., and Takigawa, T. (1987) *Chem. Scr. 27*, 135−136.
35. Palamarczyk, G., Lehle, L., Mankowski, T., Chojnacki, T., and Tanner, W. (1980) *Eur. J. Biochem. 105*, 517−523.
36. Lehle, L., Haselbeck, A., and Tanner, W. (1983) *Biochim. Biophys. Acta 757*, 77−84.
37. Wilson, I. B. H., Taylor, J. P., Webberley, M. C., Turner, N. J., and Flitsch, S. L. (1993) *Biochem. J. 295*, 195−201.
38. Forsee, W. T., McPherson, D. T., and Schutzbach, J. S. (1997) *Eur. J. Biochem. 244*, 953−958.
39. Tomita, S., Inoue, N., Maeda, Y., Ohishi, K., Takeda, J., and Kinoshita, T. (1998) *J. Biol. Chem. 273*, 9249−9254.

40. Maeda, Y., Tomita, S., Watanabe, R., Ohishi, K., and Kinoshita, T. (1998) *EMBO J. 17*, 4920−4929.
41. Stilber, H., Stephani, U., and Kutsch, U. (1995) *Neuropediatrics 26*, 235−237.
42. Freeze, H. H., Marquart, M., and Patterson, M. (1999) *Glycoconjugate J. 16* (4−5), S41.
43. Korner, C., Knauer, R., Stephani, U., and Marquart, M. (1999) *EMBO J. 18*, 6816−6822.
44. Brockhausen, I. (1993) *Crit. Rev. Clin. Lab. Sci. 30*, 65−151.
45. Brockhausen, I., Schutzbach, J. S., and Kuhns, W. (1998) *Acta Anatom. 161*, 36−78.

BI0003240